CALCULATION OF SOIL DISPLACEMENTS DUE TO RETAINING WALL CONSTRUCTION

PETER KUDELLA AND PETER M. MAYER

Institute of Soil Mechanics and Rock Mechanics,
University of Karlsruhe,
Engler-Bunte-Ring, D-76128 Karlsruhe, Germany
kudella@ibf-tiger.bau-verm.uni-karlsruhe.de
mayer@ibf-tiger.bau-verm.uni-karlsruhe.de

(Received 4 April 2000)

Abstract: With regard to serviceability state deformations, diaphragm walls and slurry walls cause considerable soil deformations during trench construction. 3-dimensional finite element analyses are able to quantify these deformations. They are compared to measurements and to the results of simplified 2-dimensional models. The dependence of soil stiffness on the actual state can be accounted for by using a hypoplastic constitutive law. Trench geometry and construction sequence are considered as factors of influence. It is shown, how the wall construction process can be modelled at the beginning of an overall 2-dimensional deformation analysis using prescribed initial deformation or stress fields.

Keywords: finite element method, soil mechanics

1. Introduction

1.1 Deformations caused during wall installation

Deep excavations in urban areas are often situated close to existing buildings, old foundations or sensitive supply pipes. Pile walls or diaphragm walls are then used as retaining structures in order to minimize deformations. Following EC 7, predictions of serviceability state deformations are required. Such predictions are commonly based on FE models, and practical reasons still restrict them to two-dimensional considerations. Most calculation methods refer to movements of given retaining structures during excavation and neglect influences from their previous installation. However, as field observations during the last years demonstrate, these deformations are by no means negligible, since they can reach up

to 50 % of the total deformations (Dibiago and Myrvoll 1972, Burland and Hancock 1977, Strobl 1982, Cowland and Thourlay 1984, Tamano 1996, Poh and Wong 1998). Therefore, they deserve accurate consideration, not only in terms of displacements, but also of the altered initial stress state left for the pit excavation. This contribution highlights the prediction of soil deformations due to diaphragm and slurry wall installation.

1.2 Wall construction and bearing behaviour

During the excavation process, the lateral stresses normal to the trench decrease to the hydrostatic pressure level of the retaining suspension. This leads to a lateral stress redistribution accompanied by increasing shear stresses forming the well-known horizontal arching effect. There are also strong indications for a predominant vertical arching at least in the lower part of the trench due to the increase of soil stiffness with depth (Ng *et al.* 1995).

For the open single trench, the only difference between the slurry wall and the concrete diaphragm wall is the suspension unit weight. Insertion of fresh concrete may lead to a reverse deformation due to its higher weight (Poh and Wong 1998), and finally to an additional reversal due to shrinking. In any case, the neighbouring trench finds a stiff support in the hardening concrete. For slurry walls, the soil arch around the new connecting trench has to brace against the stiffening slurry, which may lead to an accumulation of deformations.

1.3 Previous modelling approaches

Deformation analysis for the serviceability state in some cases refers to field tests (Fasani 1965, Strobl 1982) or to model tests (Kantartzi 1994), but the majority is derived from numerical models. Some authors regard vertical sections (Strobl 1982) or horizontal sections only (de Moor 1994), others have tried to combine horizontal and vertical plane-strain models by transferring nodal displacements from a horizontal section into a vertical section model (Ng *et al.* 1995). The majority of this research was carried out for diaphragm walls in overconsolidated clays; first results exist for slurry walls in sand (Kudella and Mayer 1998). However, it remains unsolved as how to create a realistic initial stress field for the vertical model. Furthermore, it is not clear whether any combination of initial stresses and displacements from two independent plane-strain models are able to describe reality. Only a full 3-dimensional numerical model, compared to field measurements, seems to be the appropriate approach.

2. Constitutive laws

2.1 Hypoplasticity

For FE implementation, a hypoplastic soil model is used which has proved its ability to predict the stress-strain-relation of the soil under changing stresses and densities (Gudehus 1996). It holds for a so-called "simple grain skeleton" where the stress transfer can be characterized by the mean values of grain contact forces

alone. Abrasion effects, grain fracture, macrovoids and physicochemical effects like cementation are excluded. This seems appropriate for the natural sands in Berlin. The following properties are implied:

— effective stress principle and rate-independence hold;

— the soil state is characterized only by grain pressures and void ratio;

— characteristic limit void ratios (critical, upper and lower limit, decrease with mean pressure);

— proportional strain paths lead to proportional stress paths independent of the initial state (Swept-Out-Memory).

The constitutive law calculates stress rates $\mathring{\sigma}_{ij}$ from given strain rates d_{ij}, actual stresses σ_{ij} and void ratio e. The stress rate tensor can be written (v. Wolffersdorff 1996) as:

$$\mathring{\sigma}_{ij} \approx H_1 d_{ij} + H_2 \frac{d_{ij}\sigma_{ij}}{(\sigma_{kk})^2}\sigma_{ij} + H_3 \frac{\sqrt{d_{ij}^2}}{3\sigma_{kk}}\left(6\sigma_{ij} - \delta_{ij}\sigma_{kk}\right). \tag{1}$$

The factors H_1, H_2, H_3 describing the incremental stiffness depend on the mean pressure $p_s = -\sigma_{ii}/3$ and relative density $D_p = (e_c - e)/(e_c - e_d)$. The derivation is explained elsewhere in detail. Critical, maximal and minimal void ratios e_c, e_i and e_d are uniquely related to the mean pressure according to:

$$\frac{e_i}{e_{i0}} = \frac{e_c}{e_{c0}} = \frac{e_d}{e_{d0}} = \exp\left[-\left(\frac{3p_s}{h_s}\right)^n\right]. \tag{2}$$

These equations require eight constants as material parameters: critical friction angle (φ_c), granulate hardness (h_s), minimum, critical and maximum void ratio at zero pressure (e_{d0}, e_{c0}, e_{i0}) and three exponents (α, β, n). They can all be referred to granulometric properties and determined on reconstituted samples using laboratory element tests and standard index tests (Herle 1997).

As the soil stiffness after load reversal is underestimated, an additional "intergranular strain" tensor has been introduced (Niemunis and Herle 1997) modelling smooth transitions between pseudo-elastic (cyclic loading) and full hypoplastic (monotonous deformation) stiffness. It requires further material constants and a normalized strain increment as state variables.

For FE models, this constitutive law is advantageous as there are no artificial distinctions between elastic and plastic deformations, no flow rules, and the actual stiffness is a calculation result rather than an input parameter.

2.2 Slurry stiffening

To pure bentonite suspensions a permanent stiffness can not be attributed. In numerical modelling, they may be represented by a hydrostatic pressure at the soil-wall interface. The stiffness of fresh concrete has been described by a number

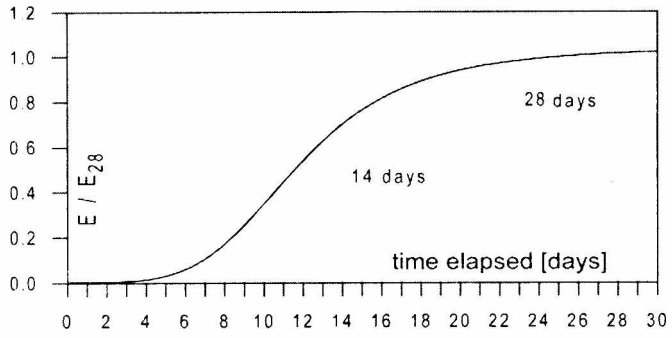

Figure 1. *Slurry stiffness vs. time*

of authors (*e.g.* Komlos 1964). However, it should be mentioned, that not only concrete hardening continues to influence the soil stress state, but also concrete shrinkage.

For slurry walls, the stiffness development of the cement-clay-suspension is of much higher importance, as cutting a new trench will reload the stiffening slurry of adjacent trenches. Laboratory and field tests have shown that stiffening occurs characteristically as shown in Figure 1. While during the first days the fresh suspension behaves like an ideal fluid, the further performance can be described using an empirical potential increase of stiffness modulus and Poisson's ratio (Nübel *et al.* 1997). Suspension dead weight is taken to be 11,55 kN/m³ for the slurry and 10,50 kN/m³ for the diaphragm wall neglecting the commonly observed increase with depth.

3. Continuous slurry wall

3.1 The SONY Center example

The SONY–Center excavation in Berlin was completed in 1998 with an average depth of 15,5 m and an area of 25000 m². The predominant wall type is a combination of a 29,30 m deep slurry wall with inserted sheet piles of 19,50 m length. The natural subsoil consists of medium dense Quarternary sands (layers A, B) overlaying a thin firm marl layer (neglected in the model) and dense Pleistocene sands (C). Both sands can be characterized by their extremely uniform and rounded grain shape. Table 1 shows the soil description, namely the representative set of material parameters and density state (expressed by relative density D_r or void ratio e_0 for zero pressure). The groundwater table is at a depth of −3,0 m. A layer of sandy debris and varying thickness close to the ground surface does not have much influence on the results.

Two measuring sections in a straight wall section have been equipped with inclinometers, deflectometers, anchor force and settlement gauges (Figure 2, described in detail by Kudella and Mayer 1998). Due to trench excavation, spatial soil displacements of up to 60-80 mm have been recorded in a distance of 4 m from the wall.

Table 1. *Soil state, granulometric and derived hypoplastic parameters of Berlin sand*

layer		A	B	C
sample depth	[m]	5	8	15
ρ	[g/cm³]	1,793	1,659	2,061
D_r		0,72	0,45	1,00
S_r		0,20	0,15	0,90
d_{50}	[mm]	0,75	0,33	0,20
U		2,74	2,40	1,75
φ_c	[°]	32	31	32
S_r	[MPa]	3730	6650	10700
n		0,20	0,26	0,24
e_{d0}	$\sim e_{min}$	0,46	0,48	0,53
e_{c0}	$\sim e_{max}$	0,75	0,81	0,84
e_{i0}	$\sim 1{,}1 \times e_{c0}$	0,90	0,97	1,00
α		0,14	0,12	0,12
β		1,0	1,0	1,0

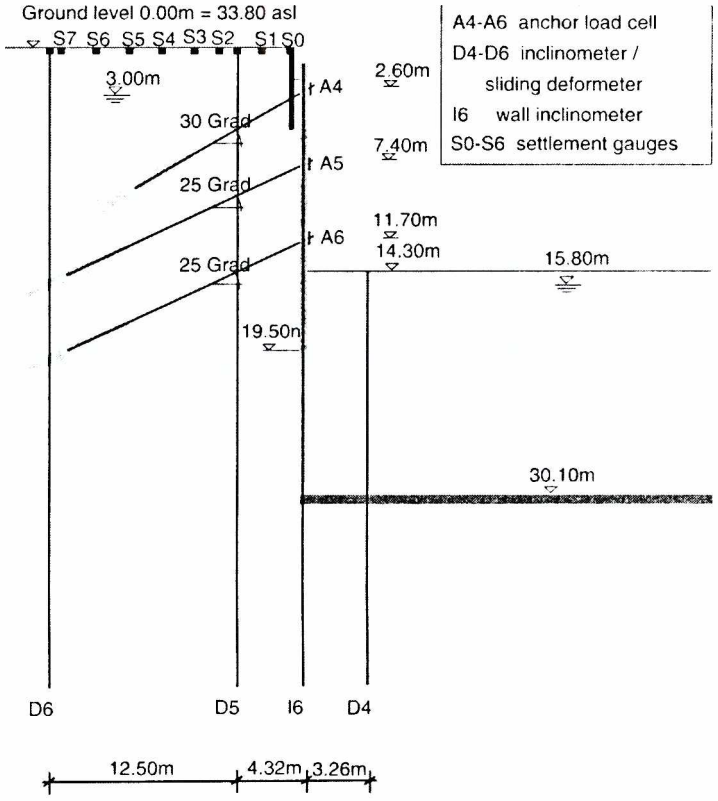

Figure 2. *Typical cross section of retaining structure and instrumentation of measuring section 2*

3.2 Numerical model

The finite element model uses the commercial code ABAQUS to which the above constitutive relations can be linked as user subroutines. The soil state is defined by the relative densities of Table 1 and by an initial stress tensor assuming Jaky's earth-pressure-at-rest.

The opening of a series of individual trenches in the calculation model follows the actual schedule of the site works (Figure 3). As the usual pilgrimstep procedure was not followed in this case, the time lag between completion of two neighbouring trenches varied between 2 and 10 days. Trench lengths are between 4,8 m and 10,8 m with an average of 7,2 m. The 3-dimensional model comprises a soil volume of 98 × 50 × 30 m using 8-node spatial elements in 11 horizontal layers (Figure 4). This model has proved to be sufficient for modelling the excavation of 8 slurry trenches with a total length of 57,6 m without boundary influences. Each trench is modelled with 2 vertical element sets. In horizontal direction, the element width is increased from the slurry wall to the mesh boundary. Normal to the boundary, the boundary nodes are fixed. The calculation follows the steps:

1. "geostatic" initial stress equilibrium;
2. guide wall installation;
3. wall excavation over the whole depth by removal of continuum elements with fixed nodes;
4. application of suspension pressure exceeding water pressure and node release;

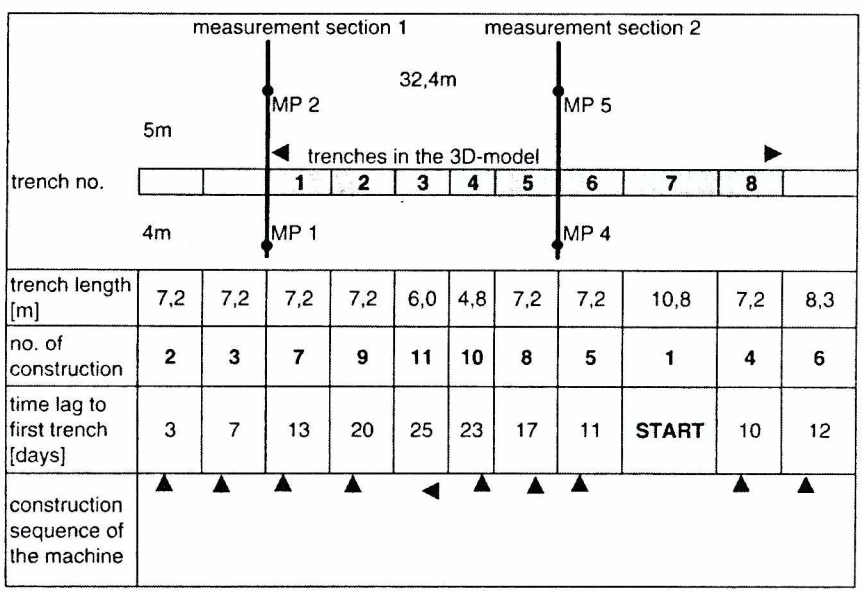

trench length [m]	7,2	7,2	7,2	7,2	6,0	4,8	7,2	7,2	10,8	7,2	8,3
no. of construction	**2**	**3**	**7**	**9**	**11**	**10**	**8**	**5**	**1**	**4**	**6**
time lag to first trench [days]	3	7	13	20	25	23	17	11	**START**	10	12
construction sequence of the machine	▲	▲	▲	▲	◀	▲	▲	▲		▲	▲

Figure 3. *Excavation sequence of the slurry wall*

5. introduction of slurry elements fixing the nodes again and keeping the suspension pressures as internal stresses;
6. modelling of breaks without production of new trenches, but with further slurry stiffening;
7. excavation of the subsequent trench repeating steps 3 to 6.

The 3D model thus requires a total of 40 steps and a calculation time of 7 hours using a high performance workstation.

Parallel to the 3D-model, also a 2D-model has been developed to represent the excavation process in a horizontal plane-strain slice in arbitrary depth. It's mesh structure in analogy to the 3D-model permits the direct comparison of results.

3.3 Comparison of prediction vs. observation

The following comparison refers to measuring section 2, if not otherwise indicated. Calculation predicts settlements of 27 mm at ground surface while approx. 35 mm were measured (Figure 6). For inclinometer D6 and between depths of −30 and −10 m, the evaluation of lateral movements reveals quite good agreement between measurements and the corresponding nodal displacements in the 3D calculation. For D4 and D5, especially in the upper part, measured calculations and also settlements differ considerably from thhe predicted ones (see Figure 5). This can be clearly attributed to two details which had been omitted in the calculation model for simplicity: 1. An existing fixed soldier-pile wall of 6 m depth, braced

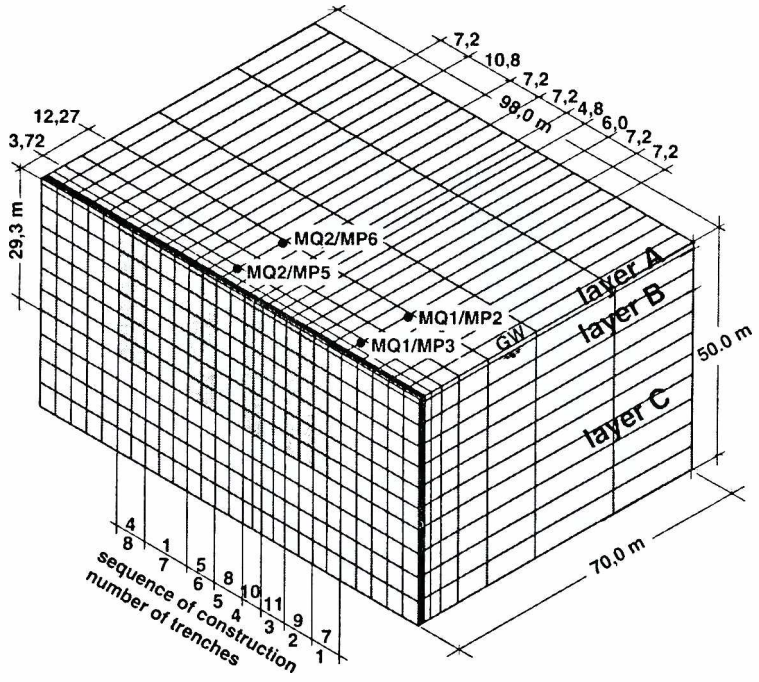

Figure 4. *3D finite-element mesh for modelling the consecutive excavation of 8 slurry trenches*

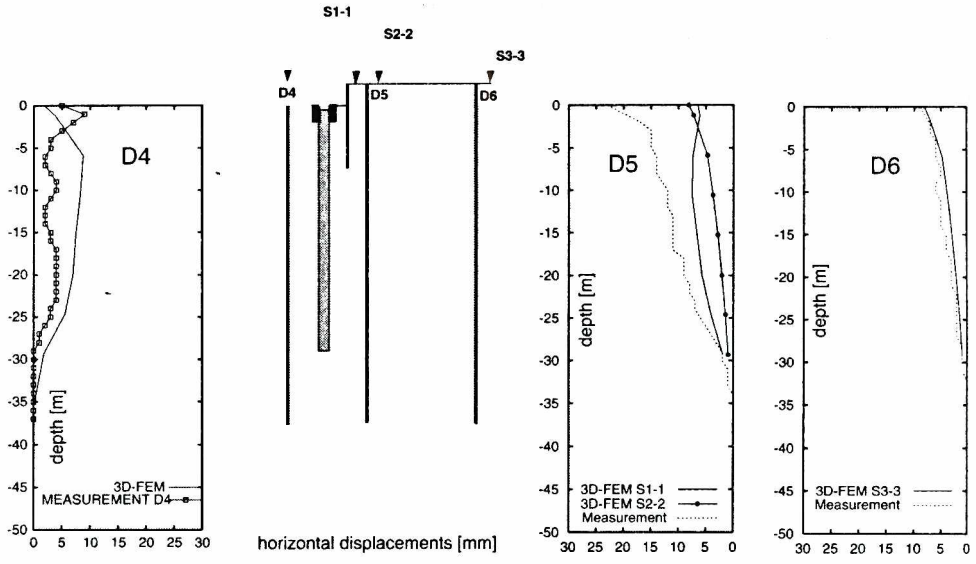

Figure 5. *Lateral displacements, measurement of 3 inclinometers (section 2) vs. 3-D-calculation*

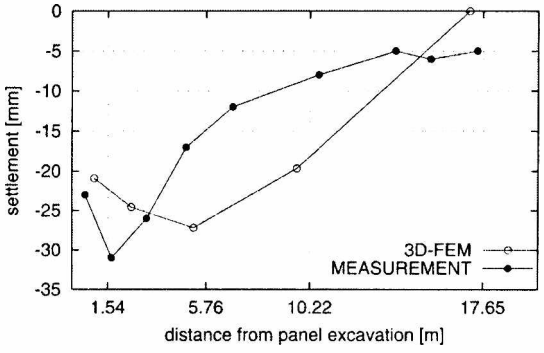

Figure 6. *Measured settlements vs. 3-D-calculation*

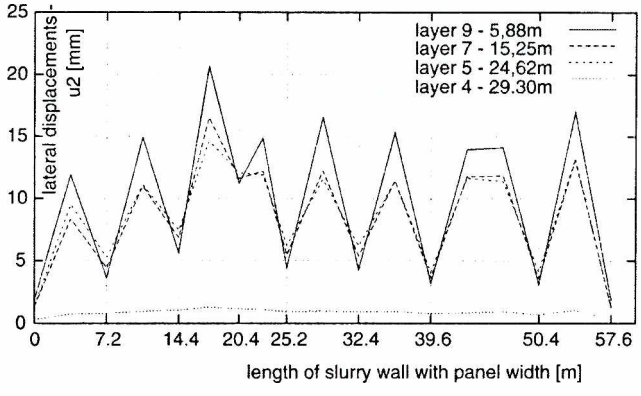

Figure 7. *Lateral displacements (horizontal sections) in different depths, 3-D-calculation*

against the guide wall, in fact acts as a row of dowels. 2. The existing 5 m wide one-sided embankment to raise the slurry level made the stiff guide wall translate laterally while the soldier piles rotated around it. Predicted displacements directly at the soil-slurry interface are distributed according to Figure 8. The magnitude of 16 to 21 mm in lateral direction could not be measured as the inclinometers were situated between two trenches in 4 m distance from the wall. The stiff "supports" of a new soil arch, made of undisturbed soil or previously filled slurry, experienced between 25 % and 50 % of the maximal lateral deformations (Figure 7) depending on the trench length and depth. With increasing depth, the displacements are smaller and more uniform, and they vanish close to the bottom of the excavation. With regard to time, most deformations occur in the first few cycles of stress redistribution. After that, additional trenches will not cause further deformations of the stiffening slurry. Also the influence of the time difference between adjacent trenches is smaller than expected.

As shown in Figure 8, the angle bounding the serviceability state deformation field is not the typical active earth-pressure inclination, but approximately 45° (according to Kantartzi's thesis 1994). At the same time, there is no constant-volume translation of the soil wedge. For both reasons, empirical approaches to predict soil deformations assuming an active earthpressure wedge (Walz and Happe 1997) cannot be satisfactory.

3.4 Comparison of 3D with 2D models

If the results of the 3D-model for a representative horizontal section are compared to the results of a 2D-slice model in the same depth, there are significant differences in displacement quantities and in the extension of deforming areas

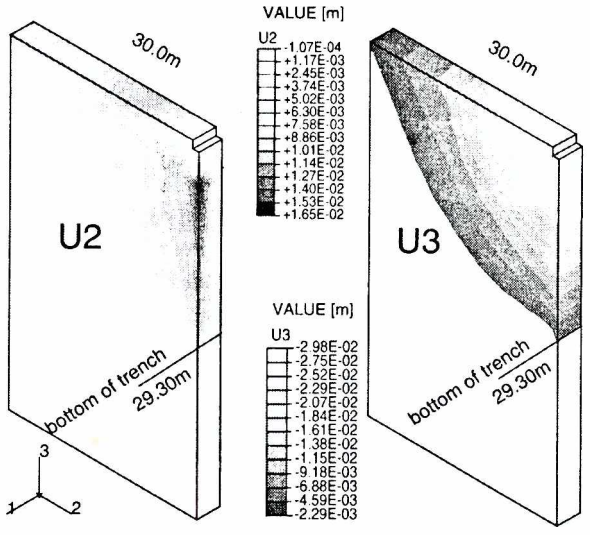

Figure 8. *Calculated lateral (U2) and vertical (U3) displacements in a vertical section, 3D-model*

(Figure 9, note that compared to the 3D-model, the 2D-model contains infinite elements, which are not shown in the figure). The 2D- model slightly underestimates lateral displacements in the upper part and overestimates them with increasing depth (Figure 10). The 2D-slice model considers only plane horizontal arching between the "supports" with a soil compressibility growing sublinearly with depth. The 3D-model, however, shows deformations concentrated in a wedge-like soil body decreasing with depth due to vertical arching.

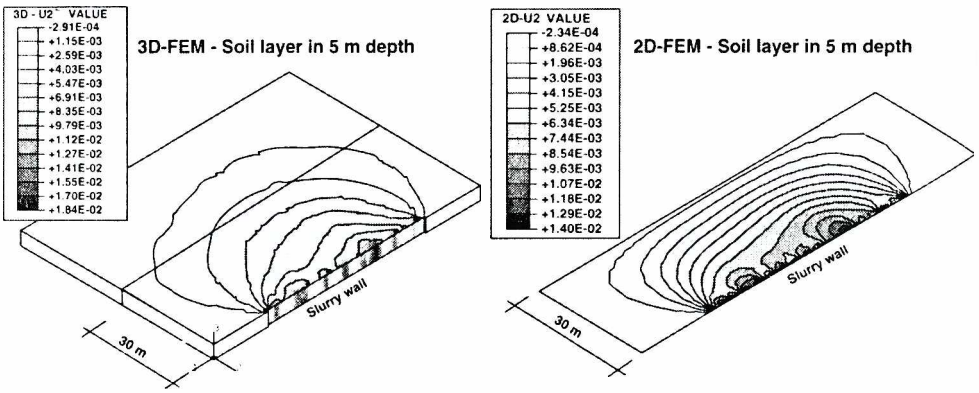

Figure 9. *Calculated lateral displacements (horizontal section), comparison of 3D-model and 2D-model in 5,9 m depth*

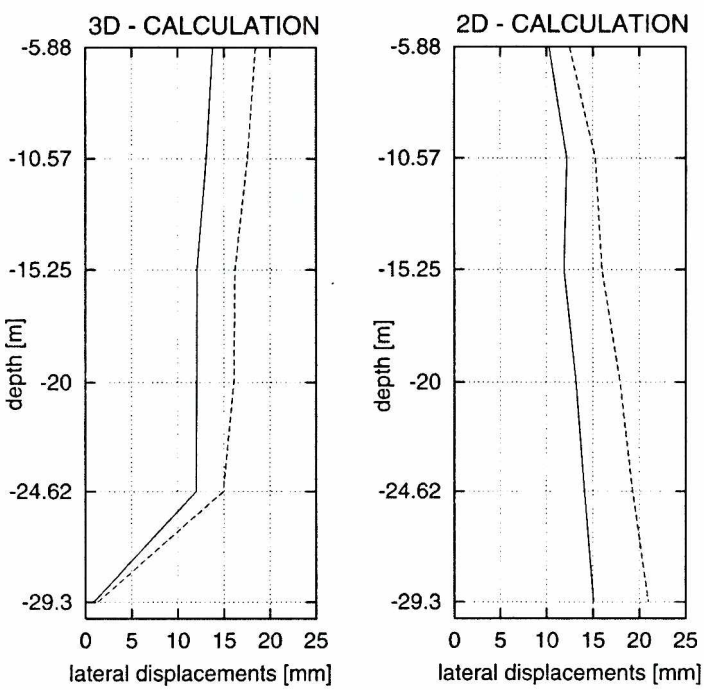

Figure 10. *Lateral displacements with depth (vertical section) — comparison of 2D and 3D calculation*

3.5 Stress redistributions

Figure 11 shows the stress history during the excavation process of the 8 trenches for two representative soil elements, one at the wall of the last trench, the other one at the adjacent support of the soil arch. In both elements, a limit state is almost reached. Elements close to the latest trench opening experience considerable horizontal stress reduction. Other elements return to their initial mean stress, but with different deviator stresses and reduced density. After that complex stress history, the initial stress state adopted for pit excavation modelling can not generally be represented by the usual K_0-assumption.

Close to the wall, arching increases the horizontal stresses by approx. 40 % at the "soil supports" and 15 % at the "slurry supports", but decreases as much as 50 % in between (Figure 12), depending on the trench lengths. If average stresses are regarded parallel to the panels, a general stress relaxation results for all depths

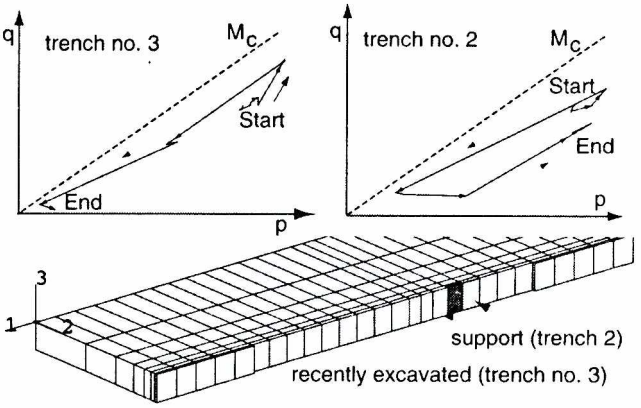

Figure 11. *Stress paths for 2 soil elements in 5.9 m depth due to 3D calculation*

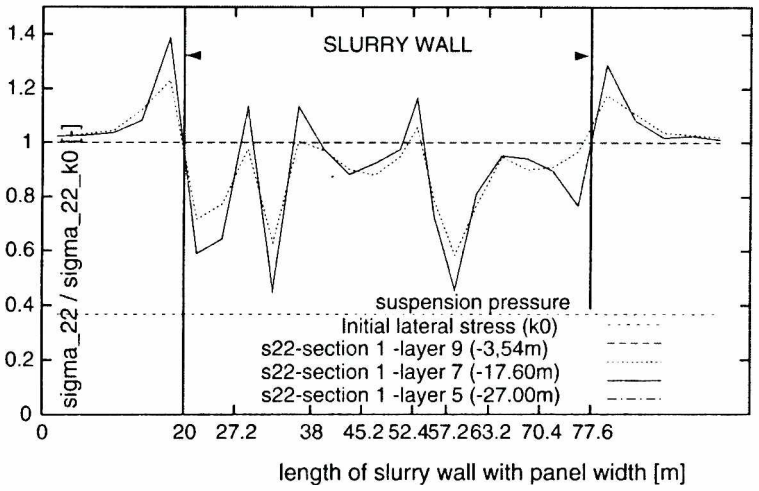

Figure 12. *Horizontal stress reduction ratios at the wall (horizontal sections) in different depths, 3D calculation*

and lateral distances. In a considerable lateral distance from the wall, *i.e.* 10 m (Figure 13), there is still a 15 % relaxation in average. While the stress fluctuations decrease with depth, this average reduction holds more or less for all depths.

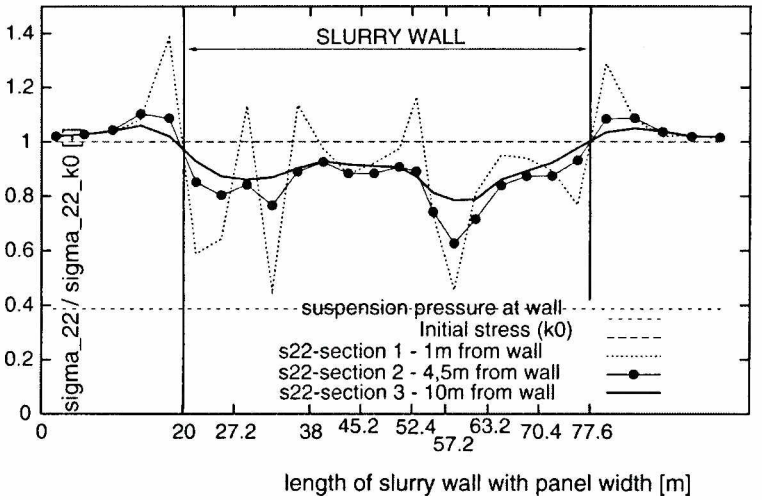

Figure 13. *Horizontal stress reduction ratio (horizontal section) in a depth of –17,6 m and different distances from the wall*

3.6 Construction sequence

The influence of the actual construction sequence is demonstrated by Figure 14. If the maximal deformation of each new trench is normalized with its length, the repeated stress redistribution in the soil is accompanied by a steady accumulation of displacements. In the light of this finding, the construction sequence (nr 7-8-6-5-4-3 according to Figure 15), which was adopted here in order to minimize settlements cannot be recommended.

Conventional excavation sequences were studied for comparison allowing 5 days for the opening of each trench. For a continuous step-by-step excavation sequence (1-2-3-4-5-6-7-8), deformations increase for the first three trenches only, thus reaching a magnitude of approx. 160 % of the single trench deformation. This can be explained by a soil disturbance acting only once at each point. For a typical pilgrimstep sequence (1-3-2-5-4-7-6-8), each soil region is disturbed twice, and more inhomogeneous deformations, though with the same limit mean value, are predicted. As evident from the calculation, there is always a significant accumulation of deformations for continuous slurry and diaphragm walls. Without consideration of the specific excavation sequence, a better prediction of the continuous wall performance can not be extrapolated from the single trench behaviour.

3.7 Trench filling

Due to our calculation model, the choice of concrete diaphragm walls *vs.* slurry makes little difference for the deformation part related to wall installation. The main deformations occur due to stress redistributions when the excavation is supported by

the fresh suspension. Only a minor part can be influenced by improving the compression properties of the trench filling. The more sensitive the soil is against loosening, the more any settlements and lateral displacements can only be reduced by shortening the trench length.

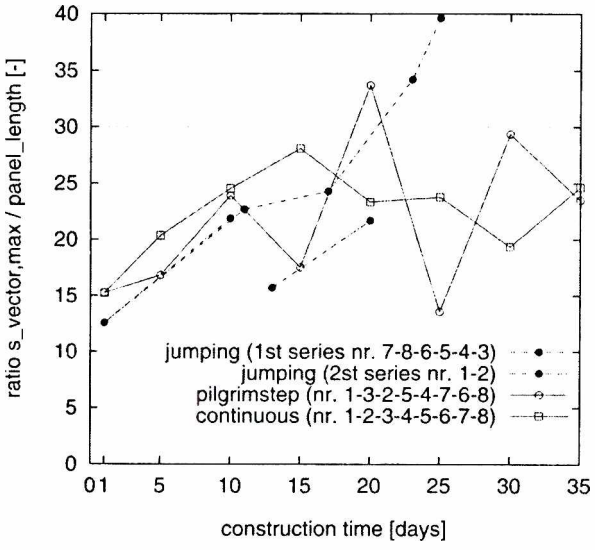

Figure 14. *Increase of normalized maximal deformation vector s_h /L × 10^4 with time for different construction sequences*

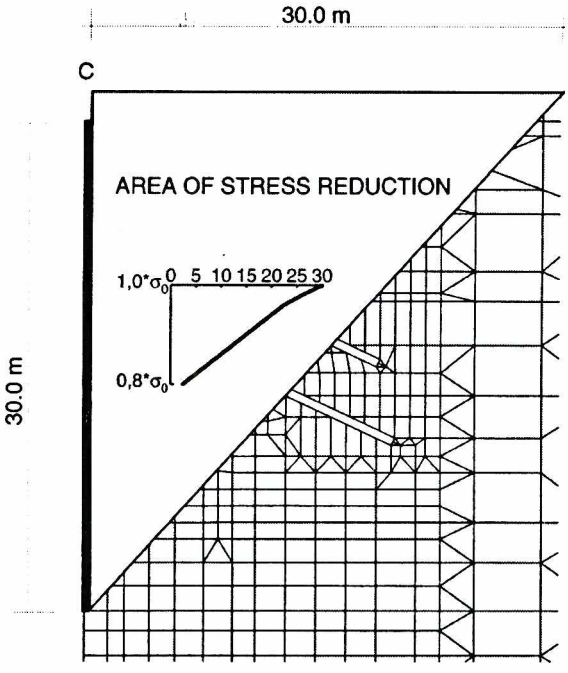

Figure 15. *Area of stress reduction shown within a 2D mesh detail and graph of the stress reduction ratio*

4. Aproximation of 3D behaviour using 2D models

4.1 Displacement approach

Conventional 2D-analyses of deformations due to pit excavation start with a K_0 initial state and thus neglect influences from the preceeding wall construction. The basic idea is the introduction of changed initial conditions into these analyses. As soil stiffness for future calculation steps is determined from stresses and strain (or density), both effects have to be included in the new initial state assumptions.

The obvious approach is the calculation of stress reductions using the FE model with a prescribed displacement profile for the wall introduced as a first calculation step after the geostatic equilibrium. A representative displacement profile in a vertical section results from average displacements at the wall-soil interface in a set of horizontal sections of various depths. From the 3D-calculation of the SONY example, constant displacement vectors with s_{hor} = 12,5 mm and s_{vert} = 12,6 mm result almost independently from depth. Apart from the soil state, these values comprise the influences of the average trench length L_m (*i.e.* 7,2 m) and construction sequence. The vanishing displacement at the trench bottom can be accounted for by a linear decrease for a length of the say $L_m/2$.

If this displacement field is applied to the vertical section of the FE model (such FE mesh for the SONY-Center excavation is shown in Kudella and Mayer 1998), a settlement trough of 14 mm maximum results, which is at least in the correct order of magnitude. The stress response in the soil mass is a uniform general reduction of 10 %, but with almost no concentration of the reduction towards the wall.

However, major shortcomings are evident, rendering the approach useless: The magnitude of stress reduction strongly depends on the FE model width, and also the resulting settlement must be arbitrary. Provided a general correction factor for the initial displacement could be found for a specific geometry modelling a realistic stress reduction close to the wall, the isotropic initial stress field misinterprets the further behaviour of the retained soil mass. This holds at least for soil movements and bearing characteristics of ground anchors embedded in the soil mass outside the real initial-stress-reduction area (see Figure 15).

4.2 Stress reduction approach

The only alternative is the prescription of complete initial stress fields based on the stress reduction factors derived from the 3D-model. When superimposed to the K_0 initial stresses, equilibrium is lost and the "geostatic" step will produce further stress redistributions and a steady initial deformation field. If modelled properly, the reduction factors change steadily from high values at the wall to zero at some distance. The stress reduction may be idealized assuming a linear distribution from say ΔK_0 = 20 % to zero in a soil wedge limited by a 45°–line (Figure 15). Even for such a simplification the implementation for many elements is cumbersome.

For the SONY example, this approach is being tested using a program subroutine, which attributes reduced horizontal stresses to each element according to

its position. The results are not yet available. It is clear, however, that this approach can never model realistic initial deformations, because the deformation field results from prescribed stresses neglecting the density changes connected to the specific stress paths. Perhaps this shortcoming can be avoided if in addition to the stress field, an actualized density field is also prescribed in the "geostatic" step. It has to be demonstrated however, whether this can be done without numerical problems.

We anticipate that this approach to simplification is better suited to model the initial soil stiffness and hence to predict realistically further deformations due to pit excavation. However, it has to be accepted for this benefit that realistic initial displacements (*i.e.* settlements due to trench installation) cannot be introduced in addition to an initial stress and density field. The preservation of such information requires consistent 3-D modelling from the beginning.

5. Conclusions

Better predictions of serviceability limit state are necessary to reduce damage for urban excavations. Thy are possible for retaining constructions:

— Using improved constitutive laws, such as hypoplasticity, which model stress-path dependency of the soil's strain response to disturbance;

— Using realistic mechanical models of all relevant construction stages, such as wall installation, trench excavation, tie-back prestressing or injections;

— Using 3D models as long as 2D simplifications are impossible or not yet established.

This has been demonstrated for slurry wall and concrete diaphragm walls in Berlin sand, where the excavation stepping leads to different stress reductions and finally to different wall deflections and settlements.

Based on the comparison of field measurements and detailed numerical models, the question has to be followed on, which prediction error can be expected from which kind of simplification.

References

[1] Burland J. B. and Hancock R. J. R., *Underground car park at the House of Commons*, London, Geotechnical aspects. Structural Engineer, **55**, 87, 1992

[2] Cowland J. W. and Thorley C. B. B., *Ground and building settlement associated with adjacent slurry trench excavation*, 3rd Int. Conf. on Ground Movements and Structures, ed. J.D. Geddes, 723, 1984

[3] de Moor E. K., *An analysis of bored pile/ diaphragm wall installation effects*, Géotechnique, **44**, 341, 1994

[4] Dibiagio E. and Myrvoll F., *Full scale field tests of a slurry trench excavation in soft clay*, 5. ECSMFE, **1**, 461, 1972

[5] Fasani M., *Experimenti e misure per la stabilitá dei fabbricati interessanti dalla construzione della Metropolitana die Milano*, L'Ingegnere **41**, 229, 1965

[6] Gudehus G., *A comprehensive constitutive equation for granular materials*, Soils and Foundations, **36**, 1, 1996

[7] Herle I., *Hypoplastizität und Granulometrie einfacher Korngerüste*, diss., Veröff. des IBF, Universität Karlsruhe, Heft 142, 1997

[8] Kantartzi C., *Ground movements during diaphragm wall installation in clays*, Diss, Queen Mary and Westfield College, London University, 1994

[9] Komlos K., *Tensile Strength Investigation of Fresh and Hardening Concrete*, RILEM Symposium Trondheim, 1964

[10] Kudella P. and Mayer P. M., *Calculation of deformations using hypoplasticity demonstrated by the SONY–Center excavation in Berlin*, Int. Conf. on Soil-Structure Interaction in Urban Civ. Eng. Darmstadt Geotechnics, ed. Katzenbach and Arslan, no. 4, **1**, 151, 1998

[11] Ng C., Lings M., Simpson B. and Nash D., *An approximate analysis of the three-dimensional effects of diaphragm wall installation*, Géotechnique, **45**, 497, 1995

[12] Niemunis A. and Herle I., *Hypoplastic model for cohesionless soils with elastic strain ratio*, Mechanics of Cohesive-Frictional Materials, **2**, 279, 1997

[13] Nübel K., Mayer P. M. and Cudmani R., *Einfluß der Ausgangsspannungen im Boden auf die Berechnung von Wandverschiebungen tiefer Baugruben in Berlin*, Ohde-Kolloquium 1997, ed. D. Franke, IGT TU Dresden, Band 4, 183, 1997

[14] Poh T. Y. and Wong I. H., *Effects of Construction of Diaphragm Wall Panels on Adjacent Ground: Fiels Trial*, Journ. of Geotech. and Geoenvironm. Eng. **124**, 749, 1998

[15] Strobl Th., *Das Tragverhalten einer flüssigkeitsgestützten Erdwand neben einer Einzellast*, diss., TH Darmstadt, 1982

[16] Tamano T., Fukui S., Suzuki H. and Ueshita K., *Stability of Slurry Trench Excavation in soft Clay*, Soils and Foundation, **36**, 101, 1996

[17] Walz B. and Happe T., *Estimation of settlements of isolated footings next to suspension supported earth slits*, 15.th ICSMFE, Balkema, Rotterdam, 1443, 1997

[18] Wolffersdorff P. A., *Verformungsprognosen für Stützkonstruktionen*, Veröff. des IBF, Universität Karlsruhe, Heft 141, 1997